Cape Breton Resource Assessment

Report Submitted to OERANS

by

J. McMillan[1], G. Trowse[1], D. Schillinger[1], A. Hay[1], and B. Hatcher[2]

[1]Dalhousie University
[2]Cape Breton University

August 22, 2012

Executive Summary

The following document was prepared for the Offshore Energy Research Association of Nova Scotia (OERANS). It summarizes the flow measurements that were made using acoustic Doppler current profilers (ADCPs) at three locations in Cape Breton: two in the Great Bras d'Or Channel (Carey Point and Seal Island Bridge), and one in the Barra Strait (near Iona). The measurements at Seal Island Bridge and Barra Strait were recorded over the duration of a month using a bottom mounted 600 kHz ADCP beginning in November 2011 and April 2012, respectively. These two deployments were conducted by Dalhousie University. The measurements at Carey Point were recorded for over 7 months beginning in October 2002 using a 300 kHz ADCP that was situated approximately 4 m above the seafloor and held in place by a taut wire mooring. The deployment at Carey Point was conducted by the Bedford Institute of Oceanography.

Of the three sites, Carey Point has the most energetic flow with horizontal currents reaching 2.8 m/s. The maximum currents at Seal Island Bridge and Barra Strait were 1.9 m/s and 1.1 m/s, respectively. Furthermore, the vertical velocities at all three sites exceeded 4 cm/s during some tidal cycles. The vertical profile of the horizontal currents at Seal Island Bridge and Barra Strait were used to determine the bottom friction coefficients during both the flood and ebb phases of the tide. The Barra Strait values were in agreement with the canonical value of 0.003, whereas the Seal Island Bridge values were an order of magnitude larger which suggests the possibility of turbulent flow in the boundary layer.

This document also presents the predicted output of four typical Tidal Energy Conversion (TEC) devices at each site. The TEC devices were assumed to be passive yaw devices with a water-to-wire efficiency of 0.4. Recognizing that these assumptions result in estimates greater than a realisable value, we compare the average daily energy production, maximum power output and operating time for the devices. The predictions indicate that an optimal 10 m diameter turbine could produce over 1000 kWh per day at the Carey Point ADCP deployment site. Given a Feed-In Tariff (FIT) rate of 60 cents/kWh, the resulting gross revenue would be $600/day. At the same FIT rate, the 10 m device at Seal Island Bridge and Barra Strait would produce $110/day and $20/day, respectively, due to lower flow speeds and power density. It is important to note that the water depth at all three sites is less than 22 m; therefore, a 10 m device may prove to be unfeasible due to navigational restrictions.

1 Introduction

A summary of the ADCP deployment locations and dates are presented below in Table 1 and the positions are also indicated on the map in Figure 1. The Seal Island Bridge and Barra Strait data were collected by Dalhousie University as part of this assessment, whereas the Carey Point data were collected in 2002 by the Bedford Institute of Oceanography (BIO).

Site	Latitude	Longitude	Mean Depth	Deployment Date	Recovery Date
Barra Strait	45.9599	-60.7985	21.0 m	Apr 19, 2012	May 22, 2012
Seal Island Bridge	46.2327	-60.4881	15.1 m	Nov 25, 2011	Dec 21, 2011
Carey Point	46.2915	-60.4157	21.5 m	Oct 15, 2002	June 3, 2003

Table 1: Deployment Summary for three ADCPs in Cape Breton, Nova Scotia.

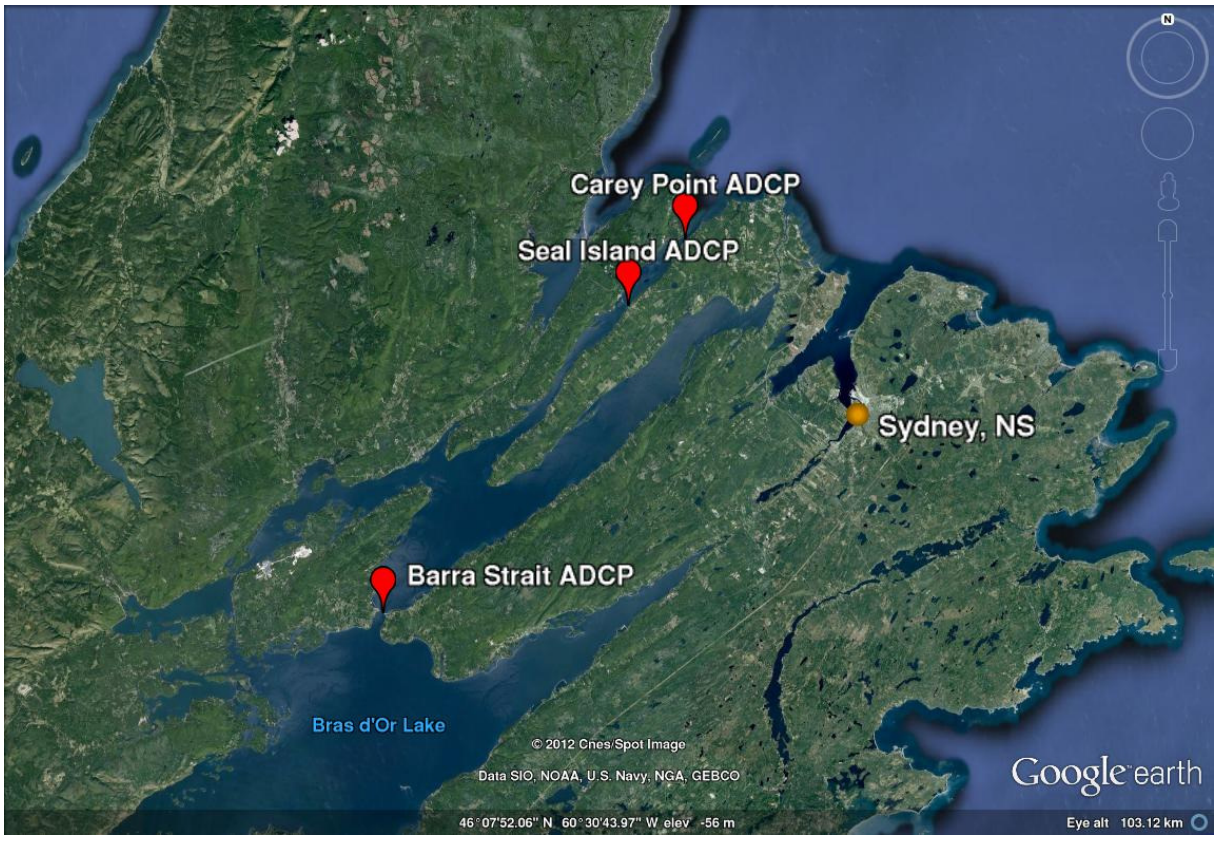

Figure 1: Locations of ADCP measurements in Cape Breton, Nova Scotia.

The structure of this report is such that each site is discussed independently – Barra Strait in Section 2, Seal Island Bridge in Section 3, and Carey Point in Section 4. For each location, the ancillary data (pressure, heading, pitch, roll and temperature), flow measurements and predicted power output are presented.

2 Barra Strait (Iona)

At Barra Strait a 600 kHz RDI ADCP was mounted on a fibreglass frame that was weighted with three 50 lb lead feet as shown in Figure 2. Ensemble averages were computed every 150 s and vertical bins were 0.5 m in size. The distance to the first bin was 2.1 m above the bottom.

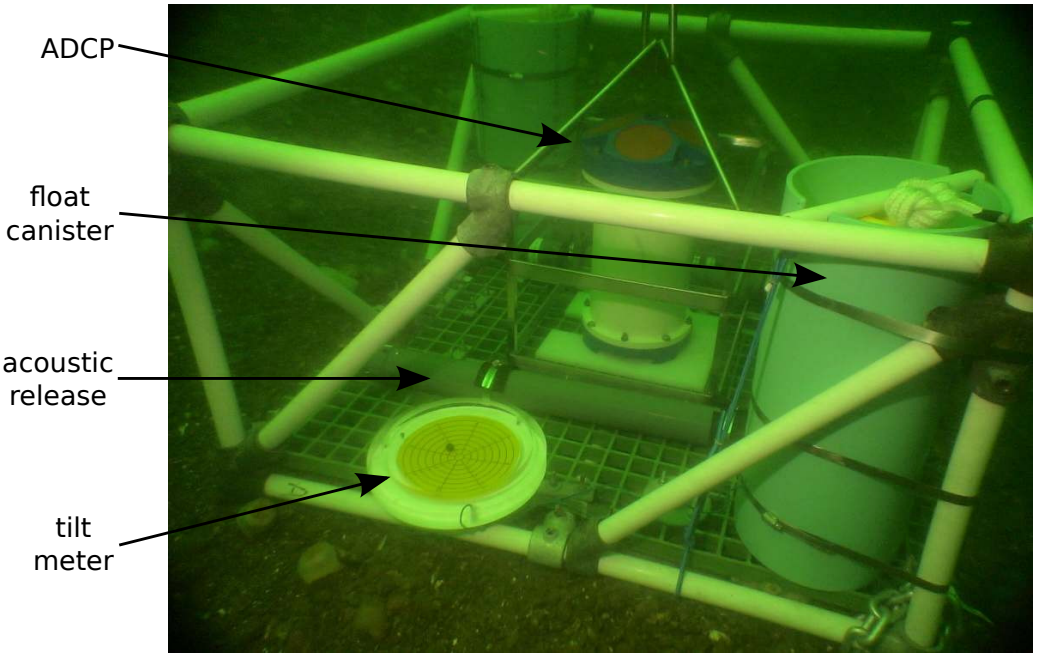

Figure 2: An underwater picture of the ADCP and its frame sitting on the bottom at the Barra Strait site. The tilt metre was removed by divers after the deployment.

The location of the ADCP is shown in Figure 3. It was positioned between the road and rail bridges, equidistant from the pylons. The nearest obstruction was approximately 15 m away from the ADCP.

Figure 3: Location of the ADCP within Barra Strait.

Ancillary Data

The ancillary data are shown in Figure 4. The time series of pitch, roll and heading all illustrate that the ADCP remained stationary throughout the deployment. Furthermore, the pressure signal incicates that the tidal range was approximately 0.5 m and the temperature signal indicates that the water temperature increased by 4°C during the deployment. The mean and standard deviation of each quantity are presented in Table 2.

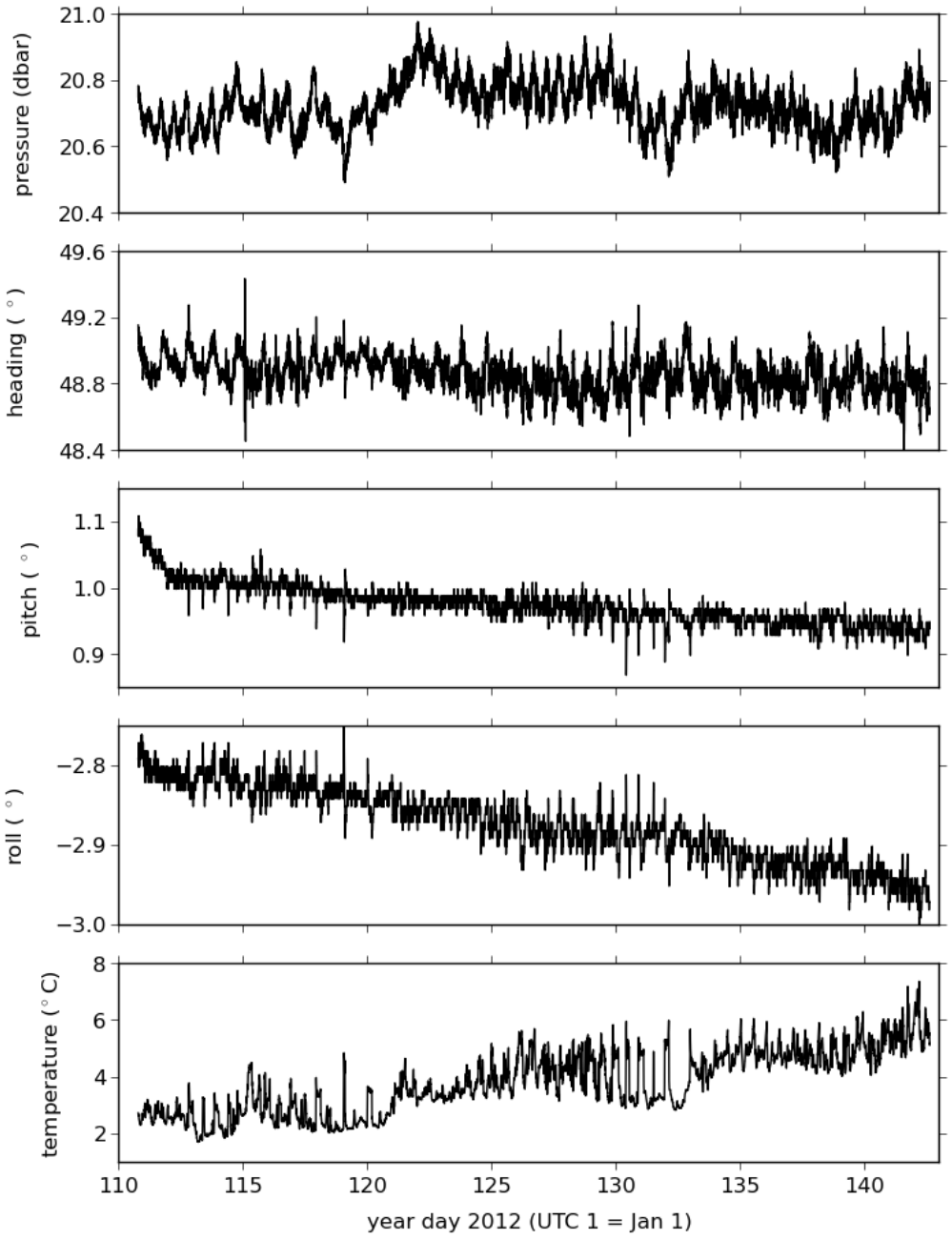

Figure 4: Ancillary data measured at the Barra Strait location.

	Barra Strait
Pressure (dbar)	20.73 ± 0.07
Temperature (°C)	3.8 ± 1.1
Heading (°)	48.9 ± 0.1
Pitch (°)	0.98 ± 0.03
Roll (°)	-2.87 ± 0.05

Table 2: Mean and standard deviation of ancillary measurements at Barra Strait location.

Flow Measurements

The ADCP flow measurements collected at the Barra Strait location are plotted in Figure 5 for the entire deployment and Figure 6 for a 2-day period. The horizontal velocities are shown in (a) and (b) in along-channel and cross-channel components, with a positive velocity representing a flood tide. The flow is predominantly in the along-channel direction, however, there is significant cross-channel flow during both the flood and ebb tides. It is thought that this displacement of the streamlines may be caused by the bridge structure. The maximum horizontal velocity at this site was 1.1 m/s and the flood and ebb tides were nearly symmetrical. The vertical velocity is shown in (c) and indicates that during the ebb tide, there is strong downward flow of 4 cm/s at this location. The error velocity, which is the difference between the two measurements of vertical velocity, is typically less than 1 cm/s as shown in (d).

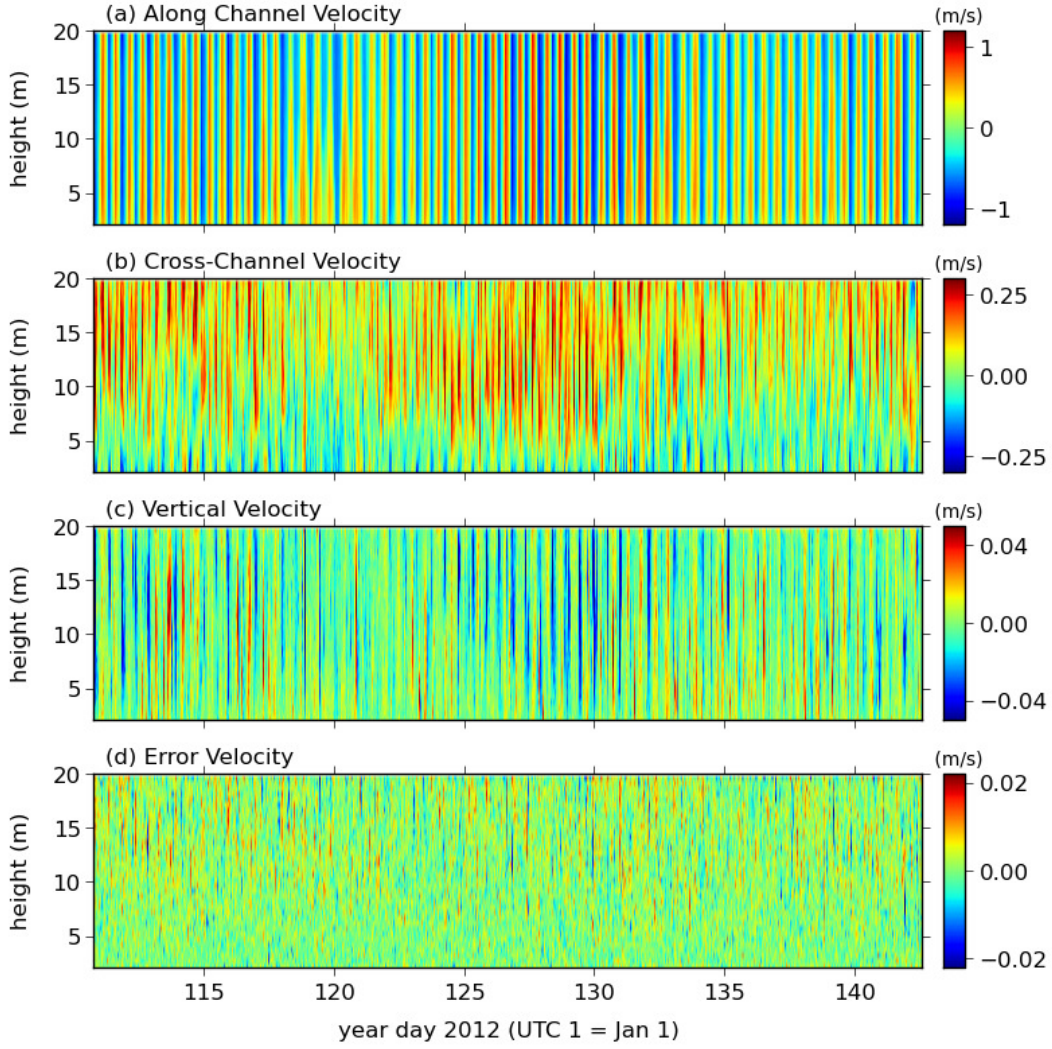

Figure 5: A complete record of the flow measurements at the Barra Strait location. Positive horizontal velocities correspond to a flood tide (i.e. south-westward flow into Bras d'Or Lake).

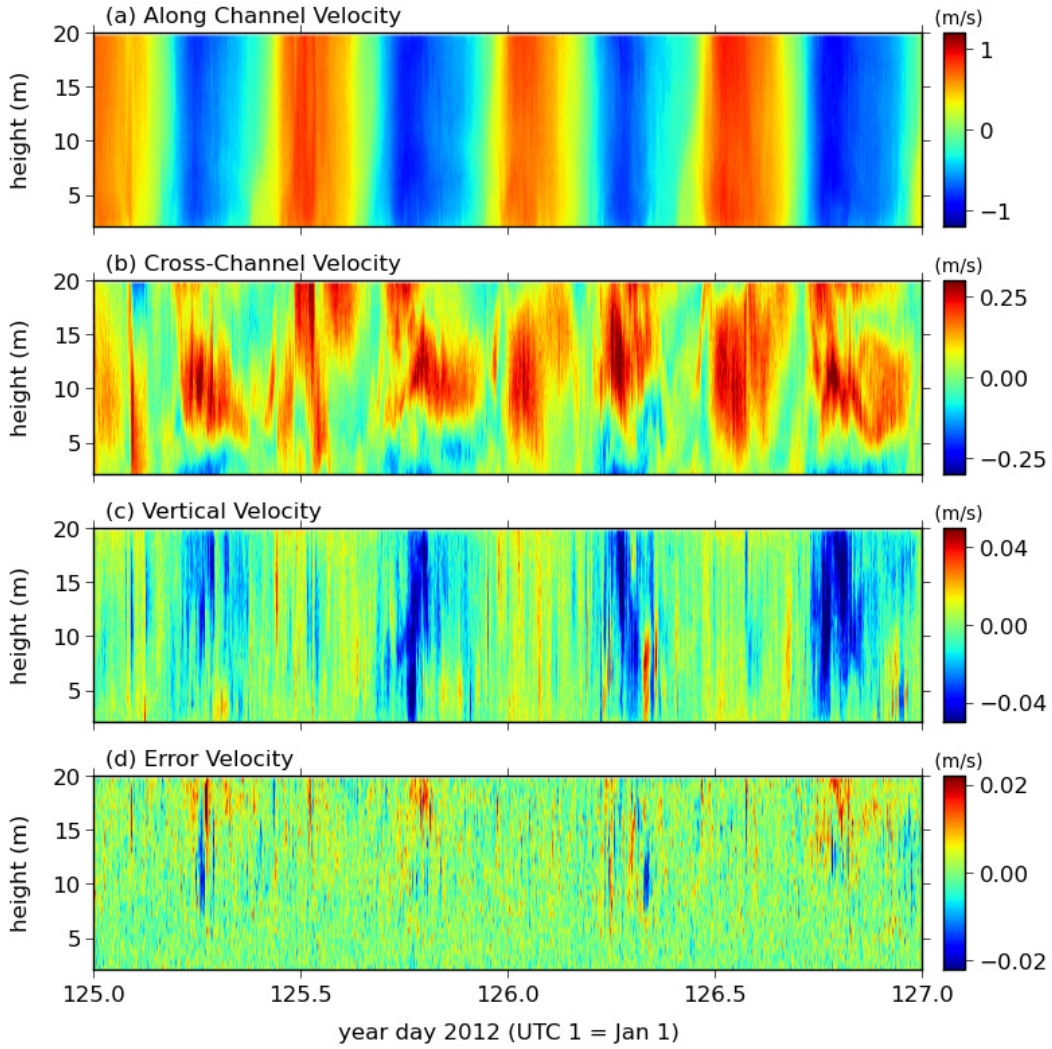

Figure 6: A two-day subset of the flow measurements shown in Figure 5 for the Barra Strait location.

From the flow measurements, the vertical profiles of the along-channel velocity were obtained at times of maximum ebb and flood. These profiles are plotted as grey lines in Figure 7. The mean of the profiles during an ebb tide is given by the solid blue line and the mean during a flood tide is given by the solid green line. The corresponding minimum and maximum profiles are illustrated by dashed lines. As expected, the flow is reduced in the bottom boundary layer.

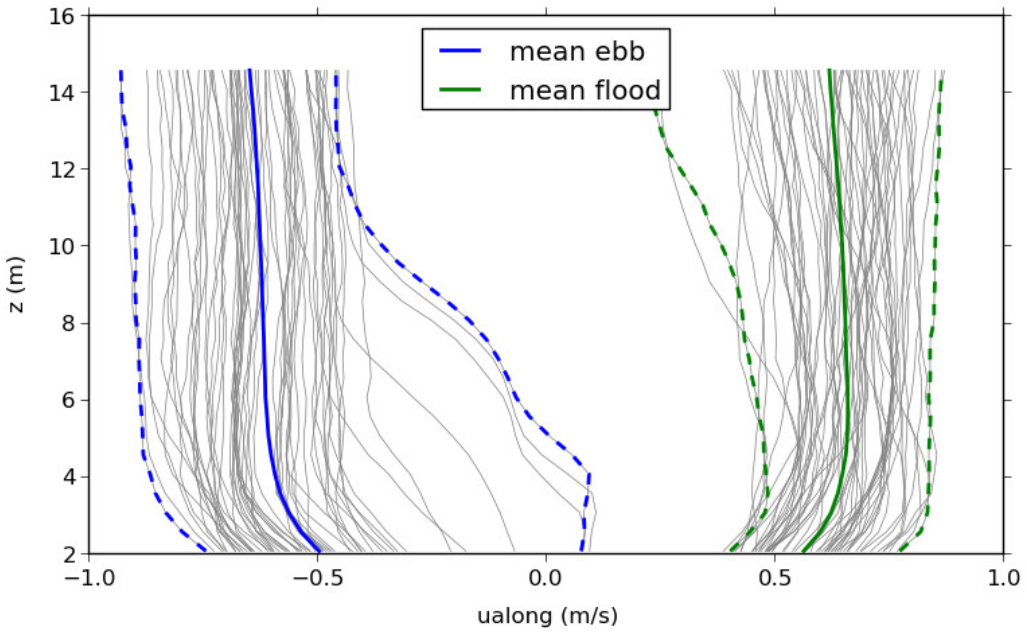

Figure 7: Vertical profiles of the along-channel velocity at the Barra Strait location. Mean profiles are represented by solid lines, and minimum and maximum profiles are plotted as dashed lines.

The bottom drag coefficient, C_d, was calculuated by assuming that the flow in the bottom boundary layer was governed by the "law of the wall" which is given by

$$u = \frac{u^*}{0.4} \ln\left(\frac{z}{z_0}\right) \tag{1}$$

where z is the height above the bottom and u is the current speed. The parameters, u^* and z_0, were detemined by fitting the above equation to the measured bottom boundary layer flow.

More specifically, the currents were averaged in 60 minute intervals and separated into ebb and flood flows. For each phase of the tide, the profiles were grouped into speed bins of 0.1 m/s intervals based on the middepth speed and an average profile for each bin was computed. Equation (1) was then fit to the bottom 4 m of each profile, resulting in estimates for u^* and z_0. The averaged profiles are plotted in blue and the corresponding fits are plotted in red in the upper panels of Figures 8 and 9 for the flood and ebb tide, respectively. From the estimates of u^*, the bottom drag coefficient was determined as the slope of u^* versus the depth averaged speed for each profile. As shown in Figures 8 and 9, this calculation resulted in a C_d value of 0.0026 during the flood tide and 0.0025 during the ebb tide which are comparable to the canonical value of 0.003.

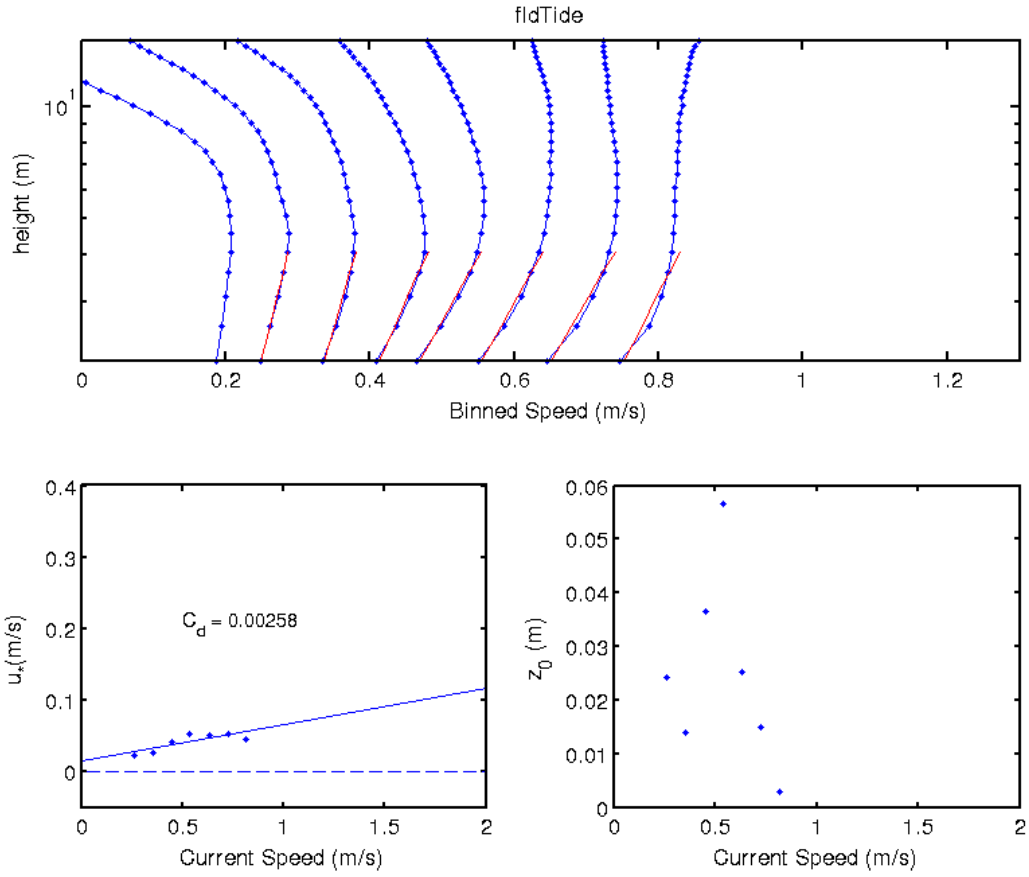

Figure 8: Law of the wall fits and the estimated bottom drag coefficient (C_d) during the flood tide at the Barra Strait location.

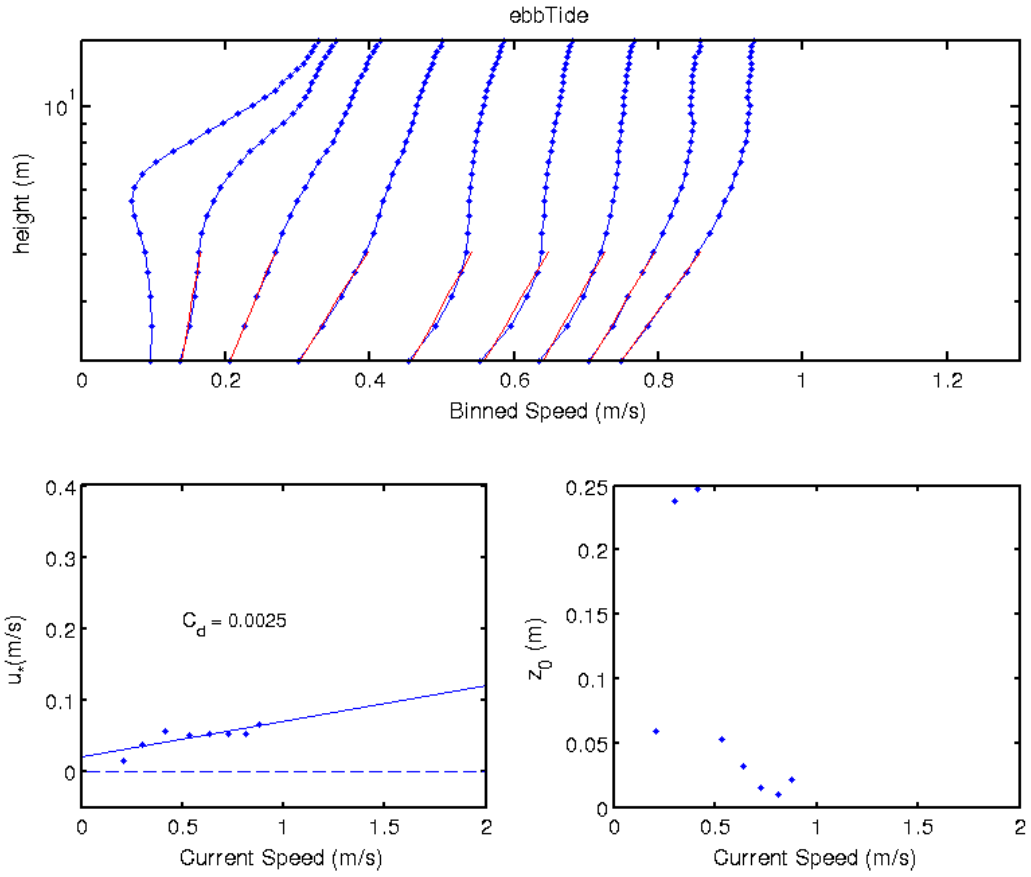

Figure 9: Law of the wall fits and the estimated bottom drag coefficient (C_d) during the ebb tide at the Barra Strait location.

During the deployment of the ADCP, a photograph of the bottom was taken (Figure 10). The seabed at this site is level, consisting of medium sized gravel. It was also noted that there was no topography exceeding 0.25 m height off the seabed within a 10 m diameter of the ADCP.

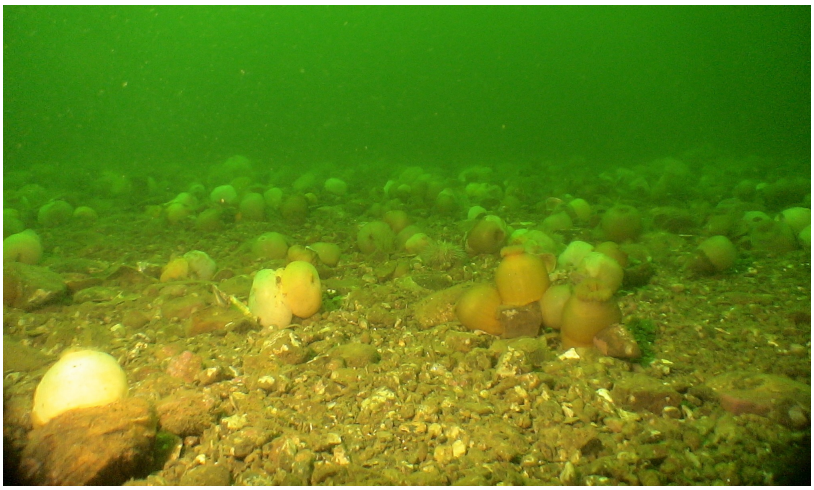

Figure 10: A picture of the seabed near the Barra Strait ADCP.

Predicted TEC Output

Using the flow measurements, the Barra Strait location was assessed for its potential power production upon the installation of a typical TEC device. It should be noted that for these calculations, a water-to-wire efficiency of 0.4 was used and it was assumed that the devices were passive yaw (i.e. the device would always align itself optimally with the flow direction). Both of these conditions likely result in overestimates of power output.

The mean water depth at the Barra Strait location was 21 m therefore a hub height of 10 m was used. The flow direction and velocity measurements at this height are plotted in Figure 11. The grey circles represent instantaneous current measurements and the solid red and blue lines correspond to the principal flow directions during the flood and ebb tides, respectively. The flow at this depth is not bi-directional in that the ebb and flood directions are less than 180° different, possibly a consequence of flow around the bridge structure. The dashed lines correspond to the standard deviations about the principal direction.

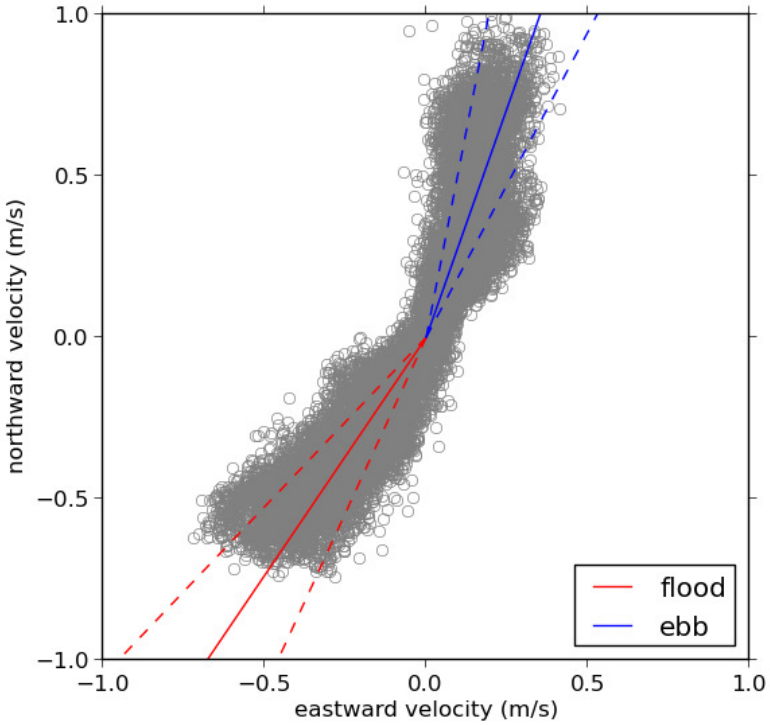

Figure 11: The principal flow directions at hub height (10 m above the bottom) are shown by the solid red and blue lines for the flood and ebb tides, respectively. The standard deviations are shown by the dashed lines and raw measurements are plotted as grey circles.

Four different configurations of turbine parameters with varying diameter (capture area) and cut-in speed were used to assess the the potential power production at the site. The turbine parameters, as well as the average energy production per day, the maximum power output and the operating time are summarized in Table 3. A time series of the power output for each turbine is also plotted in Figure 12.

Due to the low flow speeds and a cut-in speed of 1 m/s, Turbines A and C would not be operational for the majority of the month.

	A	B	C	D
Diameter (m)	5.0	5.0	10.0	10.0
Cut-in Speed (m/s)	1.0	0.5	1.0	0.5
Avg. Energy Production (kWh/day)	0.2	12.1	0.8	48.4
Max Power Output (kW)	4.6	4.6	18.5	18.5
Operating Time (%)	0.04	39.26	0.04	39.26

Table 3: Predicted energy production, maximum power output and operating time of four typical TEC devices with varying diameters and cut-in speeds at the Barra Strait location. The hub-height of the device was chosen to be 10 m.

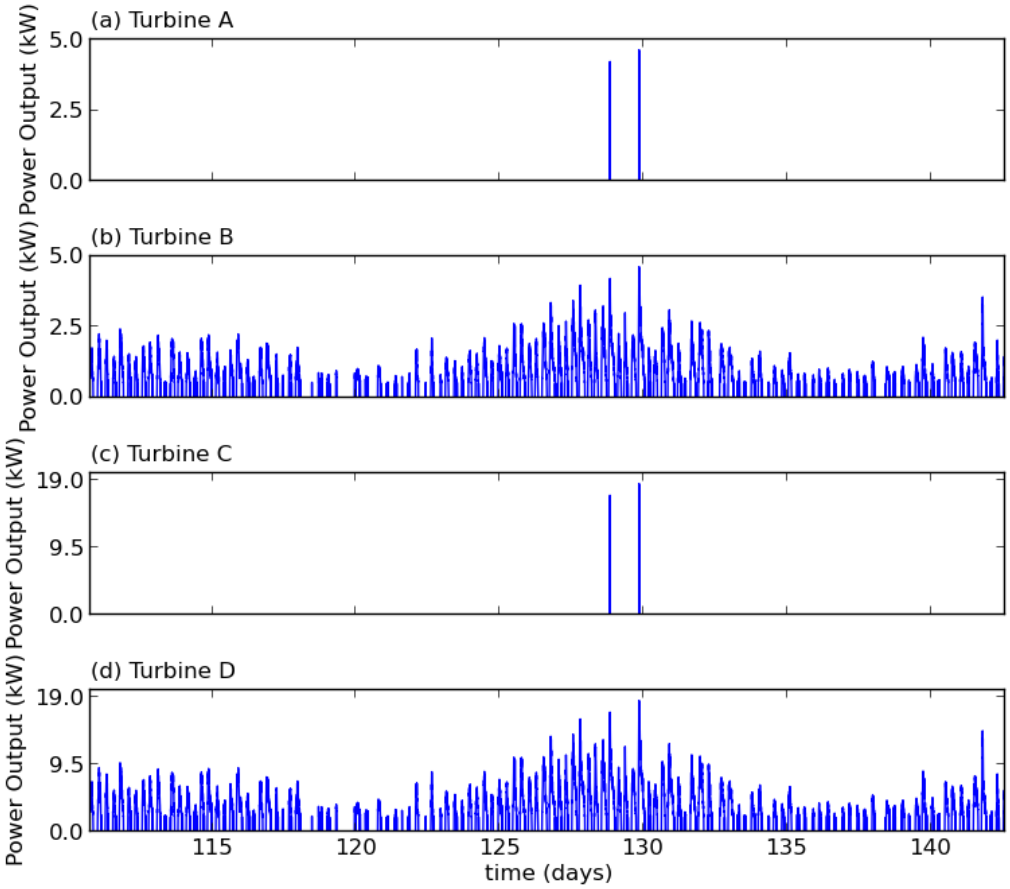

Figure 12: The predicted power output of four typical TEC devices at the Barra Strait location. The parameters for each turbine are summarized in Table 3.

Using the average energy production per day given in Table 3, the daily gross revenue is plotted as a function of FIT rate in Figure 13. This figure clearly shows that even a highly efficient turbine would produce less than $35 per day in gross revenue. It should be noted again, that these estimates are likely much higher than a realisable values.

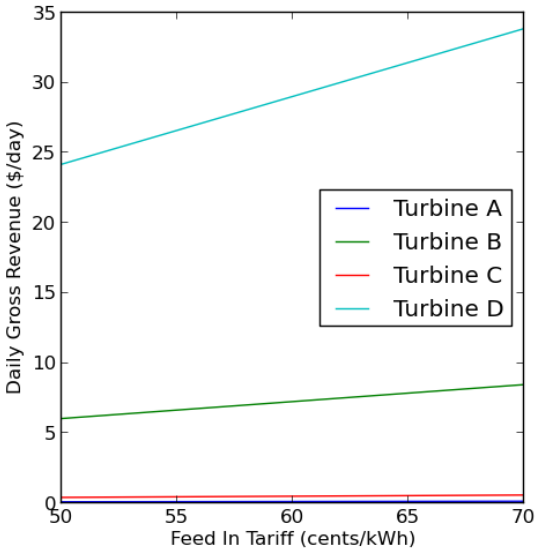

Figure 13: Predicted revenue as a function of Feed-In Tariff rate generated from four typical TEC devices installed at the Barra Strait location.

3 Seal Island Bridge

The physical configuration of the ADCP at Seal Island Bridge was identical to that used at Barra Strait (600 kHz, bottom mounted, fibreglass frame). Ensemble averages were computed every 80 s and vertical bins were 0.5 m in size. The distance to the first bin was 2.1 m above the bottom. The location of the ADCP is shown in Figure 14.

Figure 14: Location of ADCP near Seal Island Bridge.

Ancillary Data

The ancillary data are shown in Figure 15. The time series of pitch, roll and heading all illustrate that the bottom mounted ADCP remained stationary throughout the deployment. Furthermore, the pressure signal incicates that the tidal range was approximately 0.6 m and the temperature signal indicates that the water temperature decreased by 3°C during the deployment. The mean and standard deviation of each quantity are presented in Table 4.

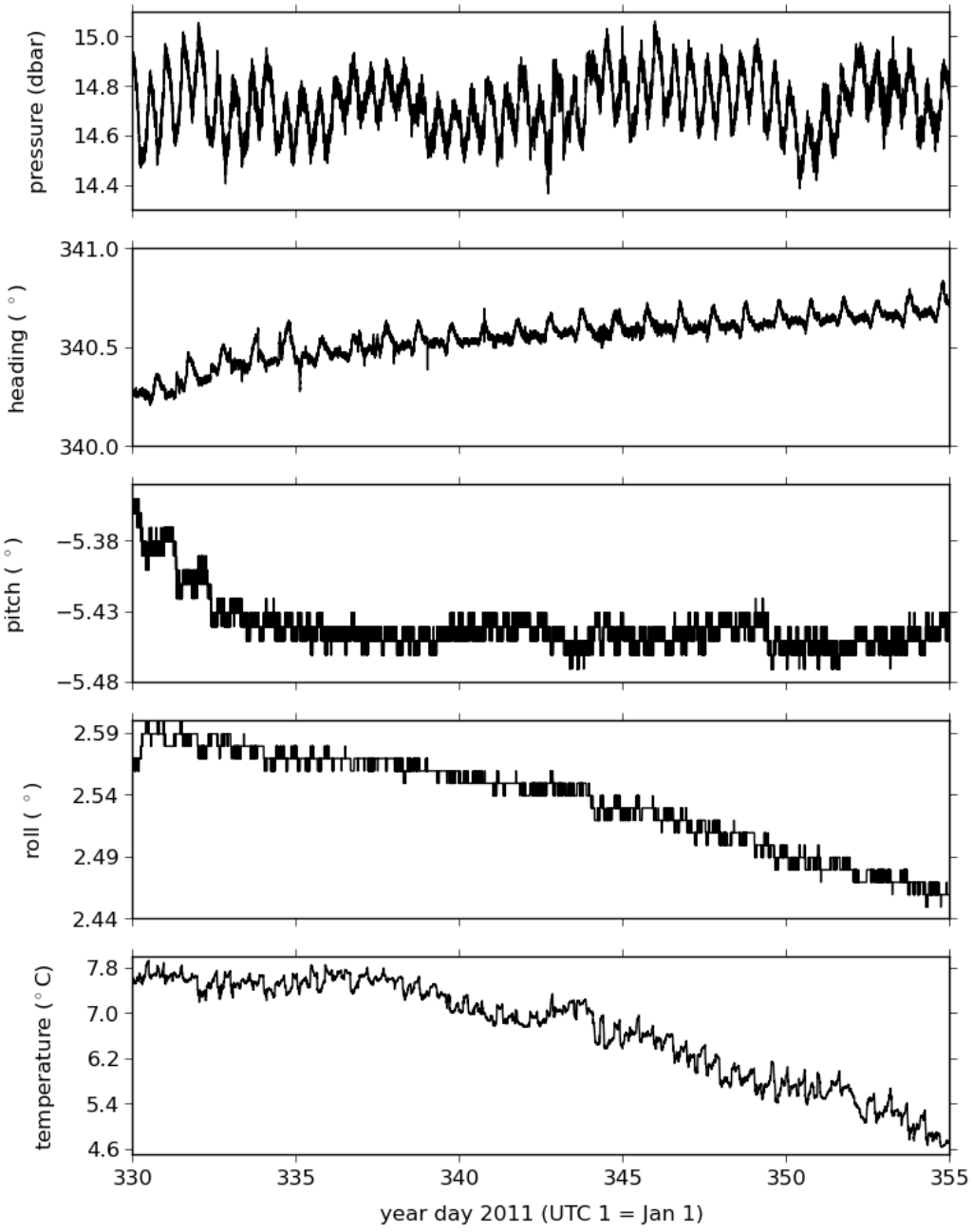

Figure 15: Ancillary data measured at the Seal Island Bridge location.

	Seal Island Bridge
Pressure (dbar)	14.73 ± 0.12
Temperature (°C)	6.7 ± 0.9
Heading (°)	340.6 ± 0.1
Pitch (°)	-5.44 ± 0.02
Roll (°)	2.54 ± 0.04

Table 4: Mean and standard deviation of ancillary measurements at Seal Island Bridge.

Flow Measurements

The ADCP flow measurements collected at the Seal Island Bridge location are plotted in Figure 16 for the entire deployment and Figure 17 for a 2-day period. The horizontal velocities are shown in (a) and (b) in along-channel and cross-channel components, with a positive velocity representing a flood tide. The along-channel velocity is about an order of magnitude larger than the cross-channel velocity. The maximum horizontal velocity at this site was 1.9 m/s and the average magnitude of the ebb flow is slightly greater than that of the flood flow. The vertical velocity and the error velocity are typically less than 4 cm/s as is shown in (c) and (d).

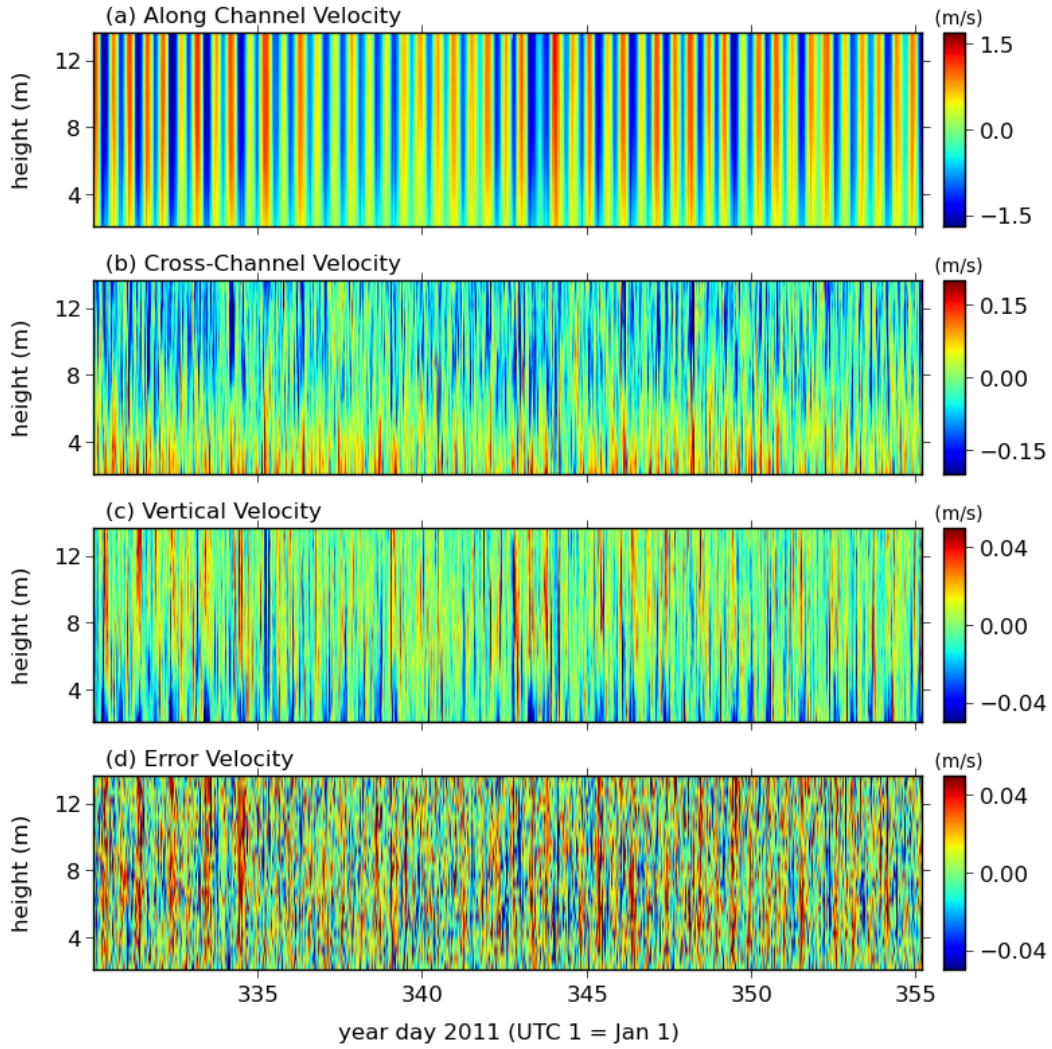

Figure 16: A complete record of the flow measurements at the Seal Island Bridge location. Positive horizontal velocities correspond to a flood tide (i.e. south-westward flow into the Bras d'Or estruary).

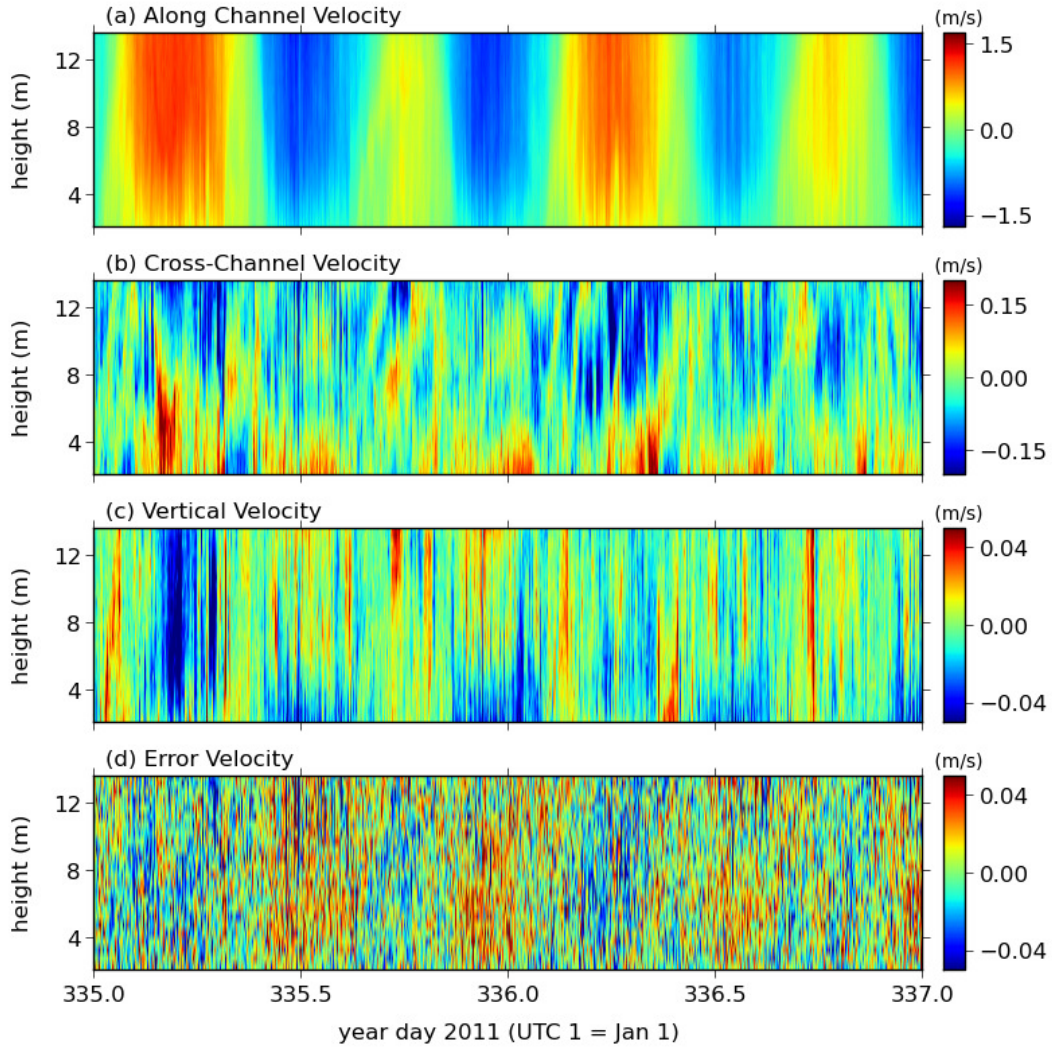

Figure 17: A two-day subset of the flow measurements shown in Figure 16 for the Seal Island Bridge site.

From the flow measurements, the vertical profiles of the along-channel velocity were obtained at times of maximum ebb and flood. These profiles are plotted as grey lines in Figure 18. The mean of the profiles during an ebb tide is given by the solid blue line and the mean during a flood tide is given by the solid green line. The corresponding minimum and maximum profiles are illustrated by dashed lines. As expected, the flow is reduced in the bottom boundary layer.

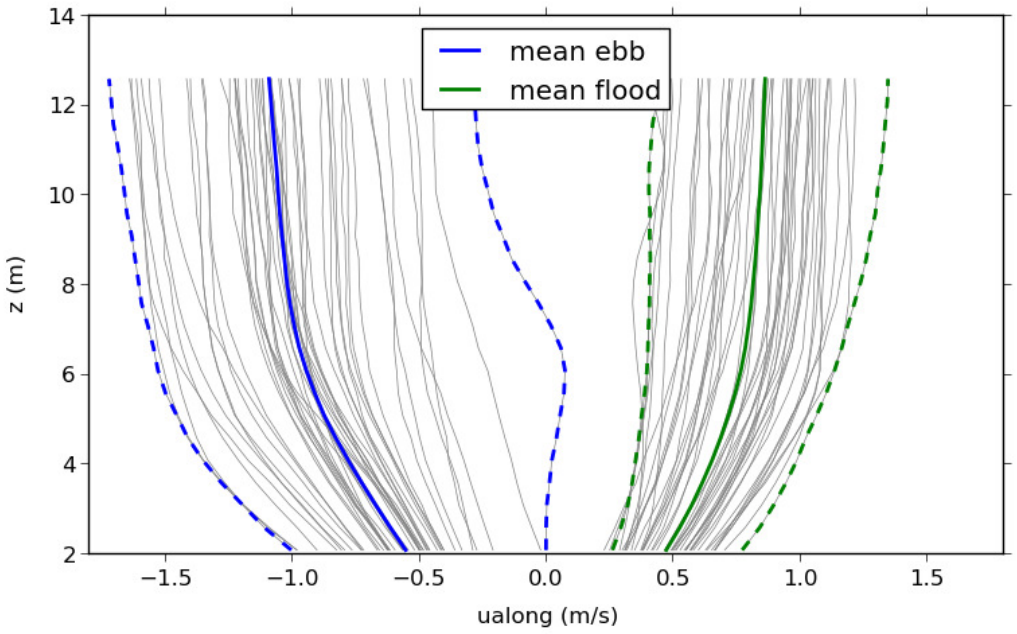

Figure 18: Vertical profiles of the along-channel velocity at the Seal Island Bridge location. Mean profiles are represented by solid lines, and minimum and maximum profiles are plotted as dashed lines.

The bottom drag coefficient was calculuated using the same methodology as described in Section 2 for Barra Strait. The law of the wall fits were performed over the bottom 4 m of the 60-minute averaged current profiles. Speed bins of 0.1 m/s were also used at this location. The averaged profiles are plotted in blue and the corresponding fits are plotted in red in the upper panels of Figures 19 and 20 for the flood and ebb tide, respectively. From the slope of u^* versus the depth-averaged current speed, the values of C_d were determined to be 0.0274 during the flood tide and 0.0215 during the ebb tide which are approximately 10 times larger than the canonical value of 0.003.

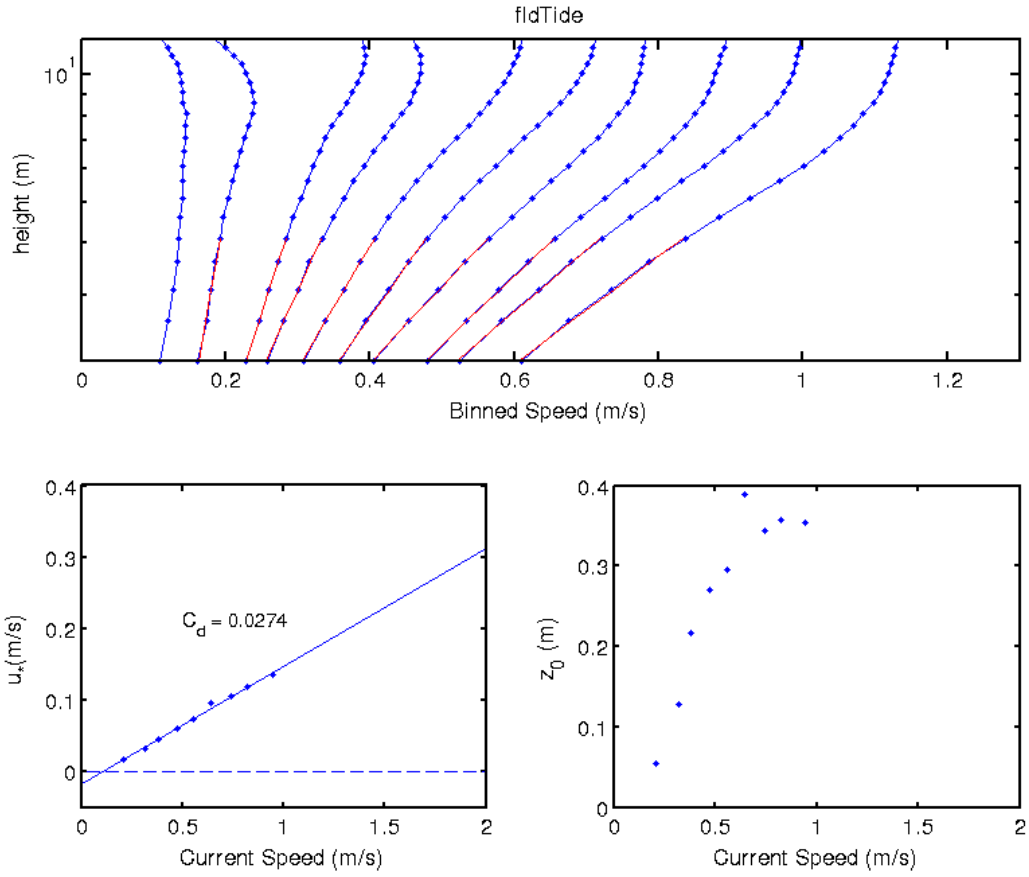

Figure 19: Law of the wall fits and the estimated bottom drag coefficient (C_d) during the flood tide at the Seal Island Bridge location.

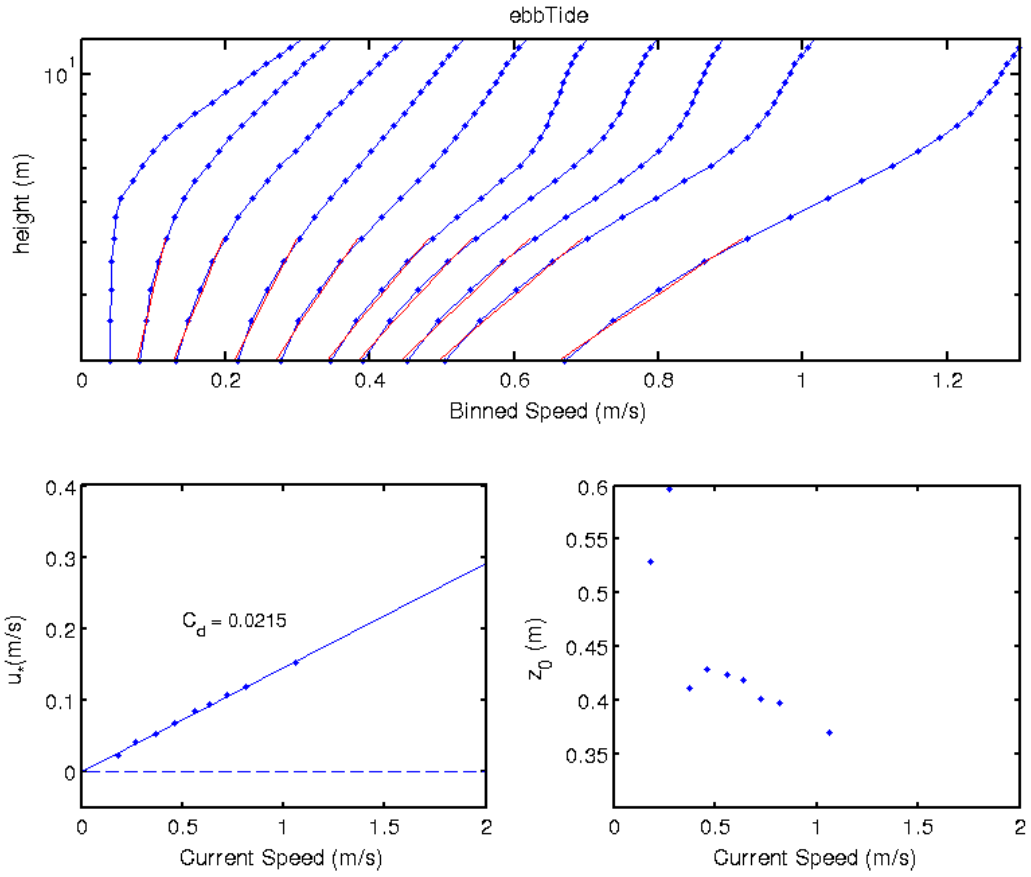

Figure 20: Law of the wall fits and the estimated bottom drag coefficient (C_d) during the ebb tide at the Seal Island Bridge location.

The seabed at this site consisted of coarse sediment over a mixture of bedrock outcrop, medium-sized rocks and coarse gravel (not shown). A bedrock ledge with a vertical drop of approximately 1 m was located approximately 4 m north of the location of the ADCP which may have generated some near-bed turbulence during the flooding tides.

Predicted TEC Output

Using the flow measurements, the Seal Island Bridge location was assessed for its potential power production upon the installation of a typical TEC device. It should be noted that for these calculations, a water-to-wire efficiency of 0.4 was used and it was assumed that the devices were passive yaw (i.e. the device would always align itself optimally with the flow direction). Both of these conditions result in overestimates of power output.

The mean depth at the Seal Island Bridge location is 15.1 m; therefore, a hub height of 7 m was used. The flow direction and velocity measurements at hub height are plotted in Figure 21. The grey circles represent instantaneous current measurements and the solid red and blue lines correspond to the principal flow directions during the flood and ebb tides, respectively. The flow at this depth is nearly bi-directional in that there is approximately 180° between the flood and ebb directions. The dashed lines correspond to the standard deviations about the principal direction.

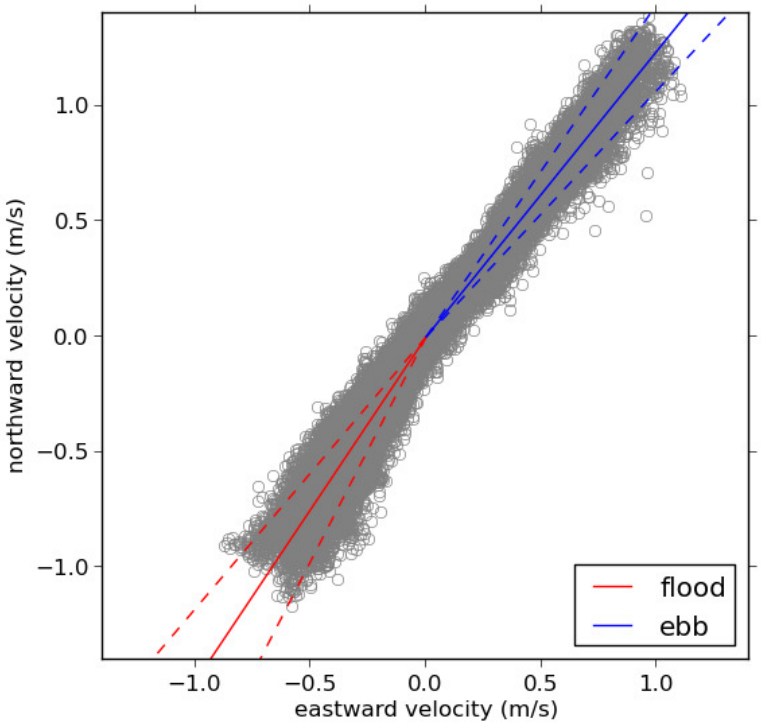

Figure 21: The principal flow directions at hub height (7 m above the bottom) are shown by the solid red and blue lines for the flood and ebb tides, respectively. The standard deviations are shown by the dashed lines and raw measurements are plotted as grey circles.

The same four configurations of turbine parameters used for the Barra Strait location were used to assess the potential power production at Seal Island Bridge. The turbine parameters, as well as the average energy production per day, the maximum power output and the operating time are summarized in Table 5. A time series of the power output for each turbine is also plotted in Figure 22.

	A	B	C	D
Diameter (m)	5.0	5.0	10.0	10.0
Cut-in Speed (m/s)	1.0	0.5	1.0	0.5
Avg. Energy Production (kWh/day)	31.7	48.2	126.9	192.7
Max Power Output (kW)	19.3	19.3	77.3	77.3
Operating Time (%)	16.58	61.16	16.58	61.16

Table 5: Predicted energy production, maximum power output and operating time of four typical TEC devices with varying diameters and cut-in speeds at the Seal Island Bridge location. The hub-height of the device was chosen to be 7 m.

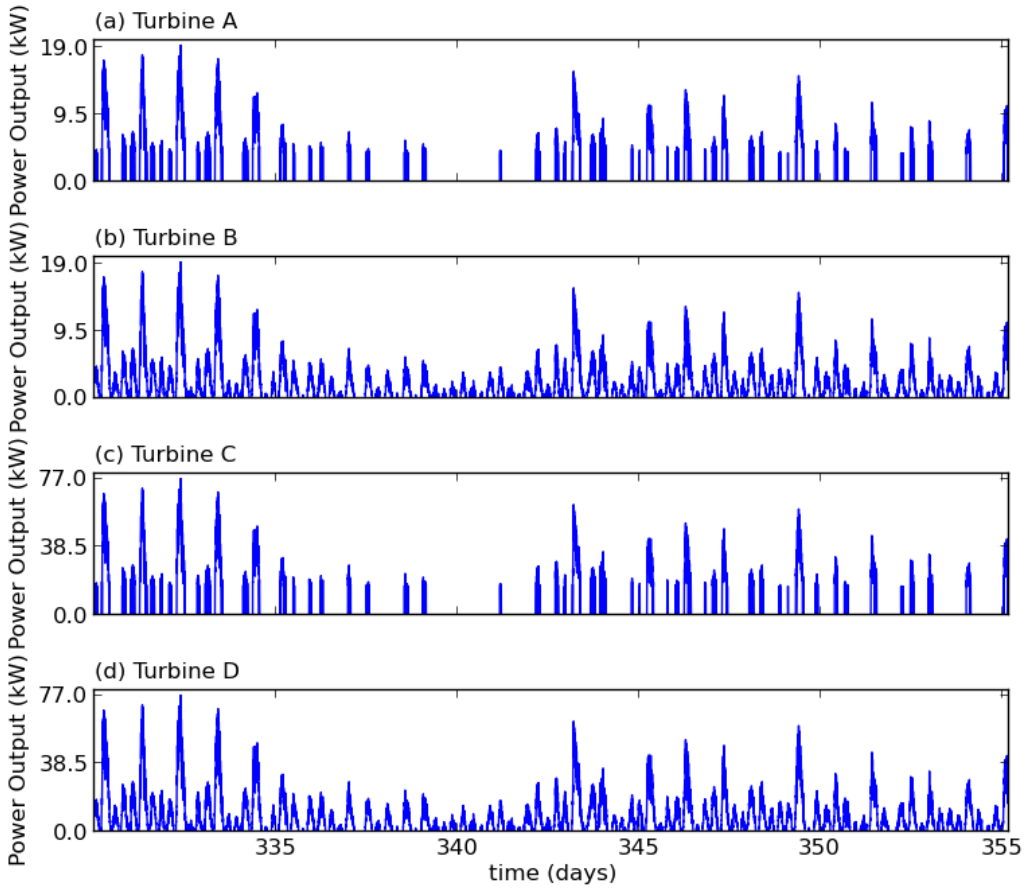

Figure 22: The predicted power output of four typical TEC devices at the Seal Island Bridge location. The parameters for each turbine are summarized in Table 5.

Using the average energy production per day given in Table 5, the daily gross revenue is plotted as a function of FIT rate in Figure 23. This figure shows that even a large, highly efficient turbine would produce less than $140 per day in gross revenue. It should be noted again, that these estimates are likely higher than a realisable value.

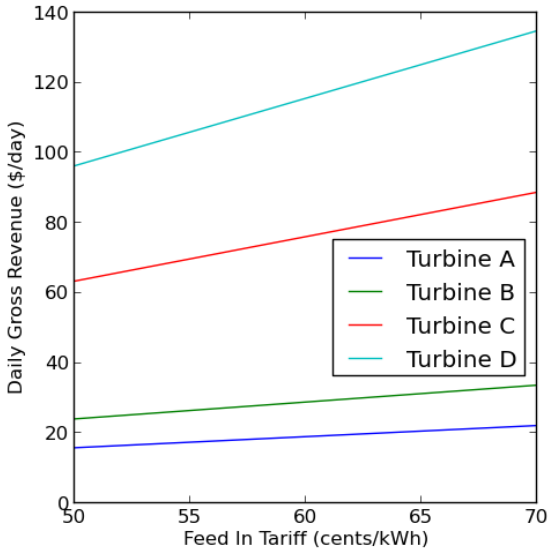

Figure 23: Predicted revenue as a function of Feed-In Tariff rate generated from four typical TEC devices installed at the Seal Island Bridge location.

4 Carey Point

The flow measurements at Carey Point were made using an ADCP that was deployed by BIO in October of 2002. The ADCP was moored to the bottom with buoyancy provided by two streamlined underwater buoyancy systems (SUBS) as depicted in Figure 24. Measurements were made every 30 minutes by averaging over a five minute window. The vertical bin size was 1 m with the deepest bin being located approximately 7 m above the bottom.

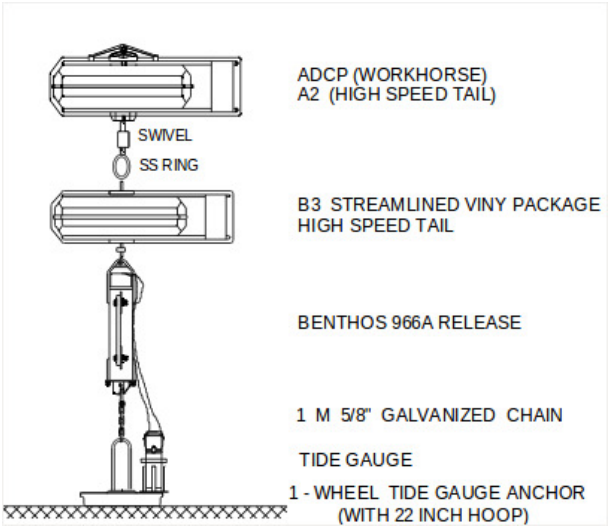

Figure 24: The mooring used at the Carey Point location. The ADCP was 3.77 m above the bottom.

The location of the ADCP is shown in Figure 25. The mean water depth at this site is 21.5 m.

Figure 25: Location of ADCP near Carey Point.

Ancillary Data

Unlike the Barra Strait and Seal Island Bridge locations, the pressure was not recorded at Carey Point. The other ancillary data are shown in Figure 26 and summarized in Table 4. The time series of heading indicates that the SUBS rotated approximately 180 degrees with each change in phase of the tide. This is expected as the SUBS is designed to align itself with the flow. The large variability in the timeseries of the pitch and roll suggest that the mooring line underwent significant movement throughout the deployment. Despite this motion, the velocity measurements were assumed to be accurate for the purposes of this report. The temperature signal illustrates the seasonal variation in the water temperature between October and June.

	Seal Island Bridge
Temperature (°C)	2.0 ± 3.7
Heading (°)	199 ± 91
Pitch (°)	6.6 ± 4.2
Roll (°)	0.4 ± 3.5

Table 6: Mean and standard deviation of ancillary measurements at Carey Point.

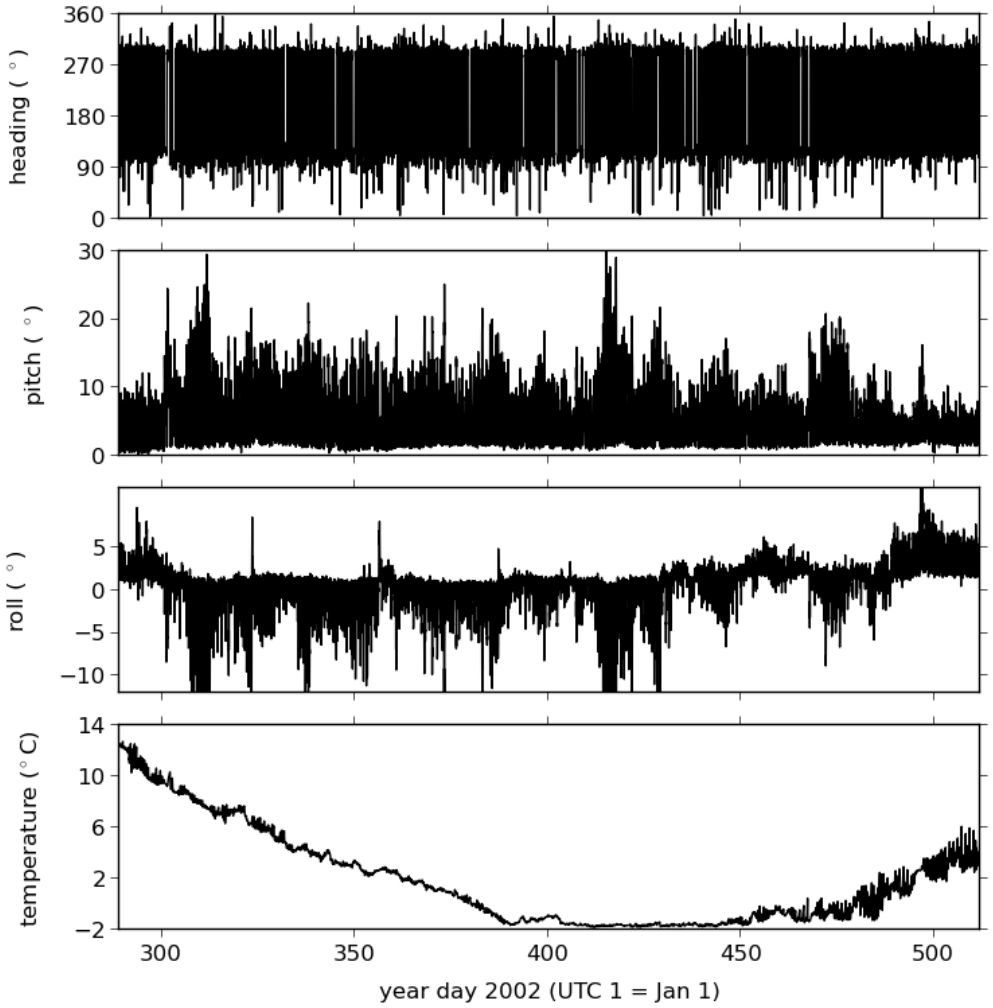

Figure 26: Ancillary data measured at the Carey Point location.

Flow Measurements

The flow measurements collected at the Carey Point location are plotted in Figure 27 for the entire deployment and Figure 28 for a 2-day period. The horizontal velocities are shown in (a) and (b) in along-channel and cross-channel components, with a positive velocity representing a flood tide. The along-channel velocity is approximately 5 times larger than the cross-channel velocity and the flow is strongest during the ebb tide. This location was approximately 60% more energetic than either Seal Island Bridge or Barra Strait locations, with the flow reaching a maximum of 2.8 m/s. The vertical velocity, which is shown in (c), is farily strong during the ebb tide and routinely exceeds 7 cm/s. The error velocity is shown in (d).

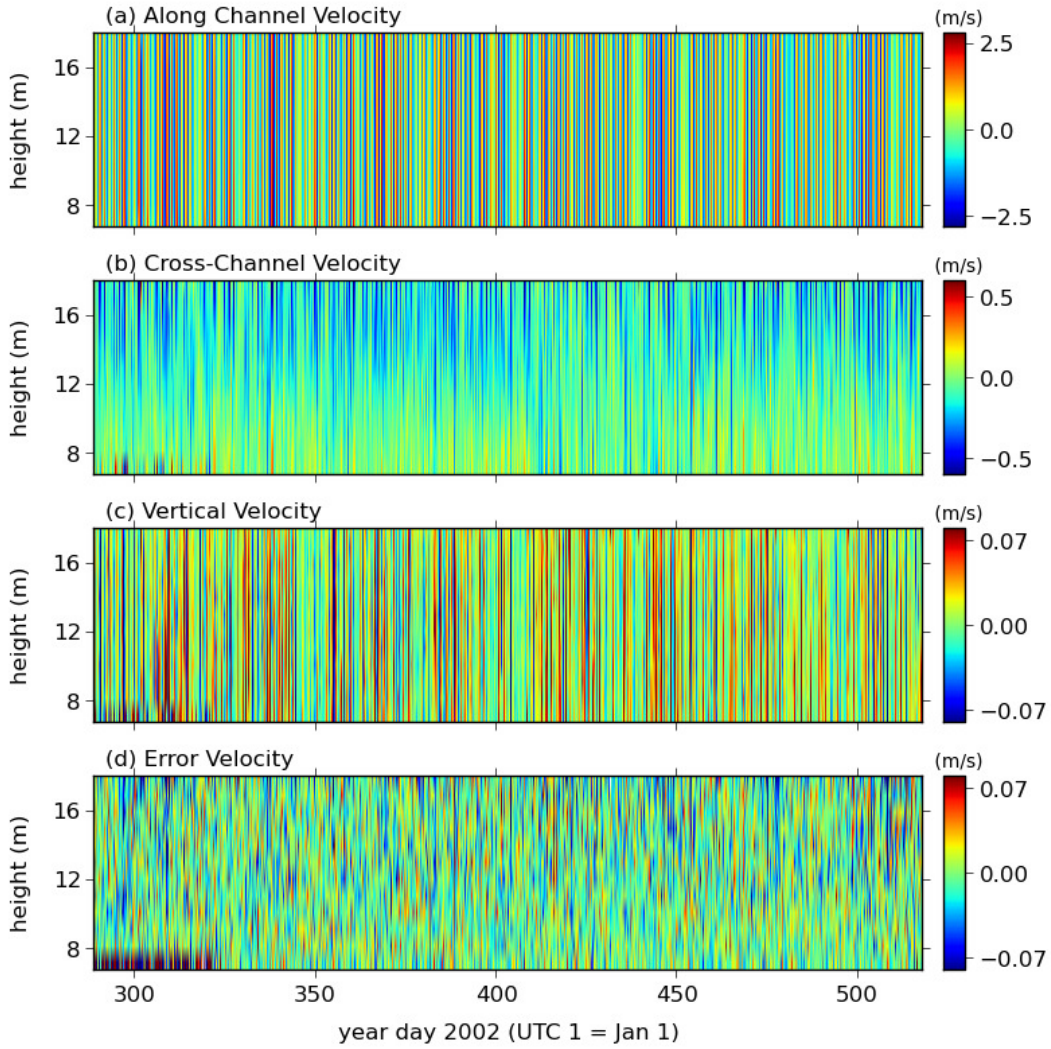

Figure 27: A complete record of the flow measurements at the Carey Point location. Positive horizontal velocities correspond to a flood tide (i.e. south-westward flow into the Bras d'Or estruary.)

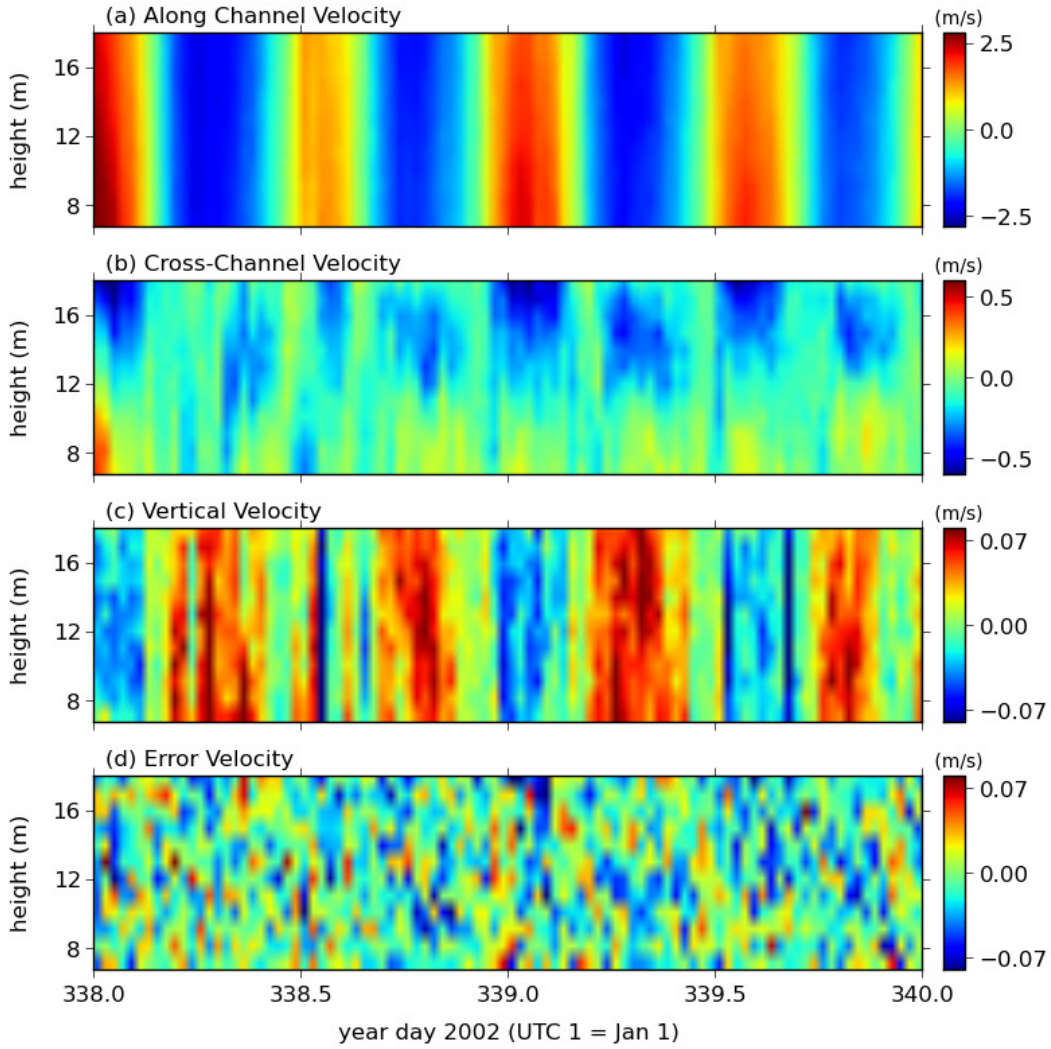

Figure 28: A two-day subset of the flow measurements shown in Figure 27 for the Carey Point site.

Due to the configuration of the mooring, the flow in the bottom boundary layer was not measured at Carey Point. Therefore, the vertical profiles are not presented and the bottom drag coefficients were not estimated for this site.

Predicted TEC Output

Using the ADCP flow measurements, this location was assessed for its potential power production upon the installation of a typical TEC device. As for the other two locations, a water-to-wire efficiency of 0.4 was used and it was assumed that the devices were passive yaw (i.e. the device would always align itself optimally with the flow direction).

The mean water depth at the Carey Point location was 21.5 m, therefore, a hub height of 10 m was used. The velocity measurements and flow direction at this height are plotted in Figure 29. The grey circles represent instantaneous current measurements and the solid red and blue lines correspond to the principal flow directions during the flood and the ebb tides, respectively. The flow at this depth is nearly bi-directional. It should be noted, however, that some variation in the flow may have been removed by the computation of 5 minute averages during data collection.

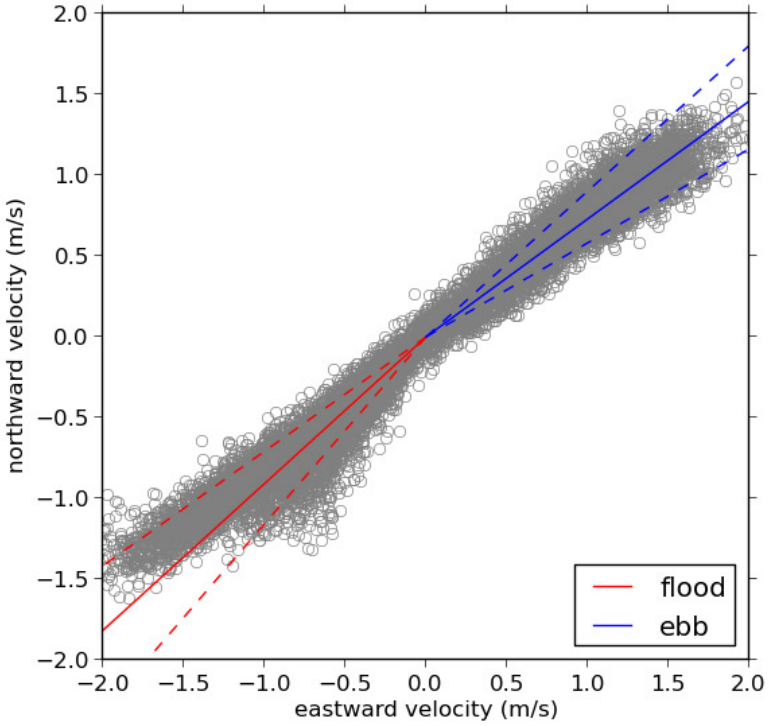

Figure 29: The principal flow directions at hub height (10 m above the bottom) are shown by the solid red and blue lines for the flood and ebb tides, respectively. The standard deviations are shown by the dashed lines and raw measurements are plotted as grey circles.

The same four configurations of turbine parameters used for the other locations were used to assess the potential power production at Carey Point. The turbine parameters, as well as the average energy production per day, the maximum power output and the operating time are summarized in Table 7. A time series of the power output for each turbine is also plotted in Figure 30. In comparison to the other two sites, the flow speeds at Carey Point regularly exceed the chosen cut-in speeds, making a turbine at this location operational for a larger percentage of time.

	A	B	C	D
Diameter (m)	5.0	5.0	10.0	10.0
Cut-in Speed (m/s)	1.0	0.5	1.0	0.5
Avg. Energy Production (kWh/day)	257.5	266.8	1029.8	1067.0
Max Power Output (kW)	91.7	91.7	366.7	366.7
Operating Time (%)	55.17	80.15	55.17	80.15

Table 7: Predicted energy production, maximum power output and operating time of four typical TEC devices with varying diameters and cut-in speeds at Carey Point. The hub-height of the device was chosen to be 10 m.

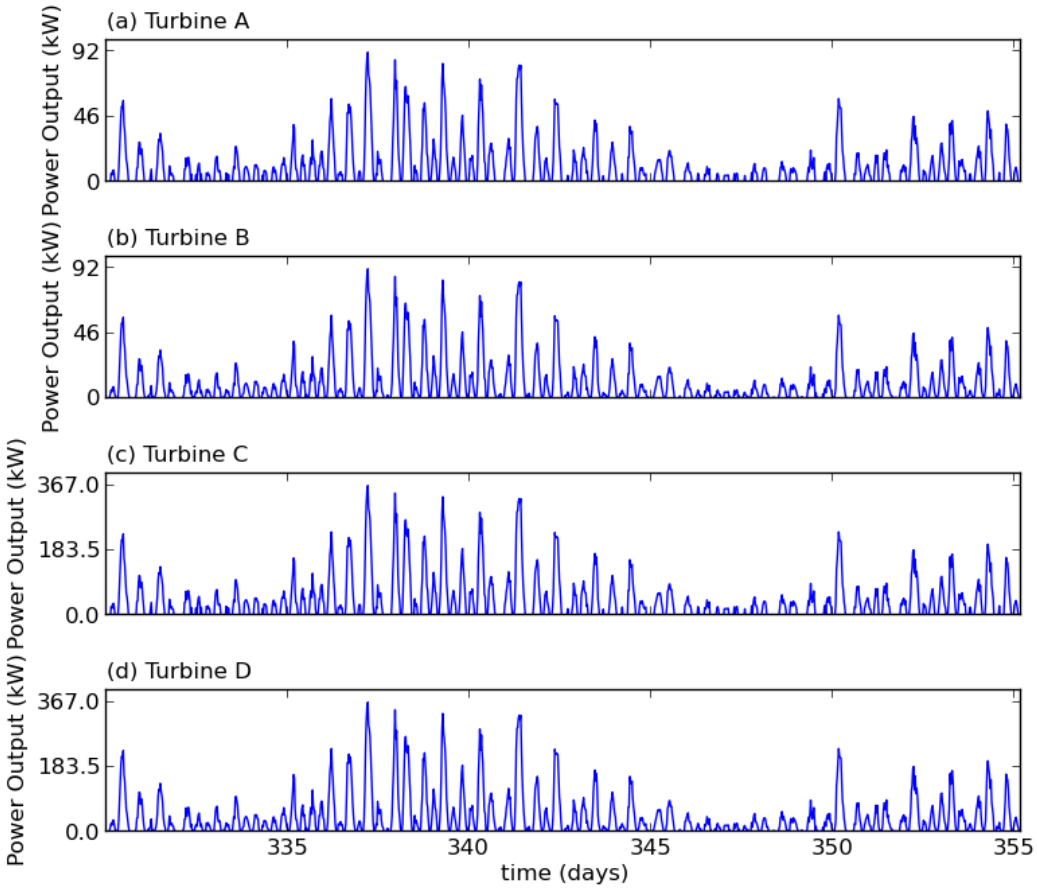

Figure 30: The predicted power output of four typical TEC devices at the Carey Point location. The parameters for each turbine are summarized in Table 7.

Using the average energy production per day given in Table 7, the daily gross revenue is plotted as a function of feed-in tariff rate in Figure 31. A highly efficient turbine with a low cut-in speed (i.e. Turbine D) could have a daily gross revenue of approximately $700 per day, however, this estimate is likely much higher than a realisable value.

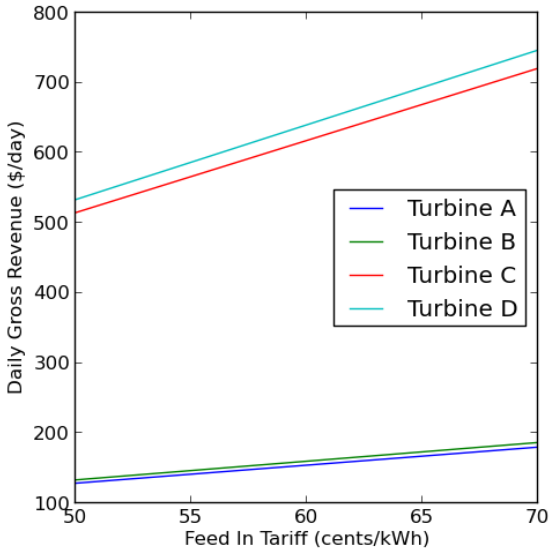

Figure 31: Predicted revenue as a function of Feed-In Tariff rate generated from four typical TEC devices installed at the Carey Point location.

5 Concluding Remarks

It should be noted that the original proposal for this project included bottom-mounted ADCP deployments at all three tidal sites discussed above. On November 25th, the Dalhousie - UCB team attempted to deploy three ADCPs, however, at the first location (Carey Point), slack tide did not occur as predicted and the deployment could not be carried out. Furthermore, due to insufficient time, only the deployment at the Seal Island Bridge location was successful. The team then returned to Cape Breton in April 2012 to conduct the Barra Strait deployment. Because of the availability of pre-existing data and a lack of additional resources, the Carey Point deployment was not conducted as part of this project.

Moving forward, we recommend that a bottom mounted ADCP be placed at the Carey Point site. The flow at this site appears to be the most energetic; however, the high-frequency, non-tidal variability in the current measurements should be taken with extreme caution. We have observed similar results in SUBS-based data from other high-speed tidal channels (Digby Gut, Grand Passage, Minas Passage) and we conclude that, while this ADCP configuration can measure general flow features, it can not be used to answer certain questions. For example, macro turbulence cannot be measured using the SUBS-moored ADCP. Another drawback of using SUBs-based ADCP data is that a large fraction of the flow in the bottom boundary layer is not measured.

Acknowledgements

We would like to thank Gary Budgen at BIO for providing us with the Carey Point data. We would also like to acknowledge Matthew Hatcher and diver John Lindley who participated in the deployment and recovery operations. Finally, this work would not have been possible without Ken Jardine of SCUBATech Ltd., and his vessel the *MV Kenworth*.